Pergamon

Int. J. Solids Structures Vol. 31, No. 14, pp. 1891–1909, 1994
Elsevier Science Ltd
Printed in Great Britain
0020–7683/94 $7.00 + .00

0020–7683(94)E0020–V

ON CIRCUMFERENTIAL SPLITTING OF A LAMINATED CYLINDRICAL SHELL

W. J. BOTTEGA
Department of Mechanical and Aerospace Engineering, Rutgers University, Piscataway, NJ 08855-0909, U.S.A.

(*Received* 9 *August* 1993; *in revised form* 2 *December* 1993)

Abstract—The problem of debonding of a laminated cylindrical shell is considered for the case where a pair of self-equilibrating line loads act through the center of a pre-existing delamination. The problem is approached as a moving boundary problem in the calculus of variations, yielding a set of self-consistent equations governing the intact laminate and governing the debonded segments of the structure, viewed both as a composite structure and individually, for this class of problems. In addition to the corresponding boundary and matching conditions, the transversality conditions which define the location of the variable boundary of a contact zone and of the delamination itself are similarly obtained. The latter results in the energy release rates which are seen to be a function of mode II or a combination of mode I and mode II fracture depending upon the presence or absence of the contact zone. A closed form analytical solution is determined and numerical results demonstrating characteristic behavior are presented. The system is seen to exhibit relatively complex behavior for the simple loading considered. General trends of the behavior of the system as a function of its material parameters, of the bond strength and of delamination size are observed.

1. INTRODUCTION

The problem of delamination growth in layered structures has received much attention, from the relatively early papers on the subject in the late 1970s and early 1980s, to the present, with an explosion in related activity in recent years. Yet, to date, most of this activity has been concerned with flat structural configurations (i.e. beams and plates). As the present paper is concerned with curved layers, the vast literature on the subject of flat structures will not be discussed here. Nevertheless, perhaps one of the earliest papers in the area was that by Kachanov (1976) which concerned itself with debonding in layered cylinders. In that paper, Kachanov determined bounds for delamination initiation for pressure loaded cylinders. In his book (Kachanov, 1988) he discussed the related problem of a partially debonded shell subjected to transverse "tensile" stresses tending to open the debonded area. This "back of the envelope" type calculation was a recasting of results from a paper published around the time of the one previously mentioned. In his calculation for a symmetrically situated disbond in an isotropic cylinder, Kachanov estimated the energy release rates and made conclusions relating to the stability of the process for the system in question.

In 1988, Bottega considered the problem of debonding of surface layers from a cylindrical substrate for the case of a contracting cylinder (Bottega, 1988a) for which the response of both inner and outer layers was considered, for the case of peeling of a layer by a point load acting at the interface of the inner surface of a cylinder and a layer (Bottega, 1988b), and the combined problem of a layer debonding from a contracting cylinder while subjected to an interfacial load simulating an imperfection or interfacial fiber (Bottega, 1988c). The three studies are summarized in Bottega (1988d). In each of the above studies results were presented in the form of growth paths in the parameter space of the system. A contact zone was assumed and growth processes were seen to be a complex combination of mode II or mixed mode (I and II) fracture involving stretching and sliding in the contact zone, as well as buckling of the delaminating layer. In each case, regions of stable, unstable and catastrophic growth were observed and these growth characteristics were seen to be dependent upon delamination size as well as on the material properties of the layer and on the strength of the bond. A related study (Bottega, 1990) was concerned with the dynamic

response of a partially debonded layer at the surface of an oscillating cylinder. Dynamic buckling of the delaminated segment and its relation to delamination growth were discussed therein.

In 1989, Chang and Kutlu (1989) considered the problem of a laminated semi-cylinder shell panel that was subjected to an externally applied and inwardly directed radial point load over the center of the debonded region. They also considered the same system subjected to external pressure acting on the outer surface of the structure. Their analysis was performed using FEM and was substantiated by parallel experiments for the case of point loading. In their analyses, Chang and Kutlu included a region of contact and concluded that such a region has substantial contributions to the behavior of the system. While most of their study was concerned with the effect of the presence of delaminations on the global buckling load of the structure, they also calculated the energy release rates for the case of pressure loading and concluded, for the situation considered, that growth was stable and mode II dominated.

More recently Larsson and Leckie (1992) have completed an interesting and comprehensive study involving composite shell panels for which the horizontal displacement at the support was prescribed and directed radially outward. They solved the problem by way of an asymptotic analysis and used their solution to calculate energy release rates for a variety of system parameters. They also examined, to some extent, the influence of bending–stretching coupling, in and out of the delaminated region, and the effect of retention (omission) of nonlinearities in their analysis. They concluded that, for the system they considered, the most critical radial location for a disbond was at the center of the laminate, and that growth was stable under the type of "loading" considered. They also intimated that inclusion of bending–stretching coupling was less critical in the delaminated region than in the undamaged portion of the panel.

Another recent investigation is that of Kardomateas and Chung (1992). In their study they considered the "thin-film" response of a delaminating layer at the outer surface of a cylindrical substrate, where the cylinder was subjected to external pressure. The analysis was performed by employing what is effectively a perturbation about the prebuckling solution in terms of assumed functional forms. Most of the study was concerned with the determination and comparison of critical buckling loads. Energy release rates were, however, calculated though neglecting geometric nonlinearities for that portion of the analysis. Based on this calculation, conclusions were drawn concerning growth of the disbond. Each of the shell studies discussed above were concerned with delaminations in plane strain and/or plane stress situations.

Finally, the extensive work of Simitses and his colleagues (Sallam and Simitses, 1987; Simitses and Chen, 1988; Chen and Simitses, 1988a, b; Simitses et al., 1991) concerning delamination buckling in shells and the influence of the presence of disbonds on the overall structural behavior must be mentioned here. In this context, the work of Troshin (1983, 1992) must be mentioned here as well. Growth of the delamination was not considered in the above analyses.

In the present study we shall be concerned with circumferential growth of a "thru" delamination situated at the interface between two thin cylinders (plane strain) or rings (plane stress) which are bonded together. In particular, we shall be concerned with the response of the system when it is subjected to radially directed self-equilibrating interfacial line loads acting at the center of the delamination. The geometrically nonlinear shell theory employed as the mathematical model for the two subcylinders is the same as that used in Bottega (1988a–d). The material properties of each individual subcylinder are not considered to vary through its thickness. The intact portion of the structure (i.e. the composite structure) will be found as a laminate of the two subcylinders, incorporating bending–stretching coupling. In the spirit of Bottega and Maewal (1983a–c) and Bottega (1983, 1988a–d, 1990, 1991, 1993), the problem will be approached as a moving boundary problem in the calculus of variations, with the boundary of the delaminated region, as well as that of a contact zone, being found as part of the solution. A Griffith type fracture criterion will also be incorporated. In this manner, the governing equations and the corresponding boundary, matching and transversality conditions will be derived and a self consistent

laminate theory will be obtained for the intact portion of the structure, for problems of this class. A closed form analytical solution will then be obtained for the case of self-equilibrating line loads. Finally, results corresponding to numerical simulations are presented, revealing characteristic behavior of the delaminating structure. It will be seen that such behavior will include lifting (separation), sliding and snap-through buckling of the subcylinders along with stable, unstable and catastrophic growth of the delamination. Regions in which the various types of growth occur will be identified in the parameter space of the system.

2. PROBLEM FORMULATION

Consider a laminated cylinder possessing a "thru" delamination over a portion of its circumferential interface and let the system be subjected to self-equilibrating radially directed line loads of intensity Q_0 acting through the center of the debonded region as shown in Fig. 1. From the type of loading considered, and from previous work involving thin cylindrical films (Bottega, 1988a–d), it may be anticipated that the inner and outer delaminated segments separate from one another and that a region of contact may exist where the debonded segments maintain sliding contact while "pushing" on one another. It will be assumed that delaminated segments possess smooth surfaces. With this picture in mind, the system may be parameterized by an angular coordinate, θ, measured positive clockwise from the center of the disbond. From symmetry considerations, only the portion of the cylinder defined on $0 \leqslant \theta \leqslant \pi$ will be considered. The system will thus be partitioned into three regions separated by the intermediate boundary angles ϕ and ϕ^*, the latter defining the boundary of the disbond. The first of these regions will be referred to as the "lift zone" or the "separation zone", and is defined on the domain $S_1 : \theta \in [0, \phi]$. As its name suggests, this is the region where the delaminated segments lift away or separate from one

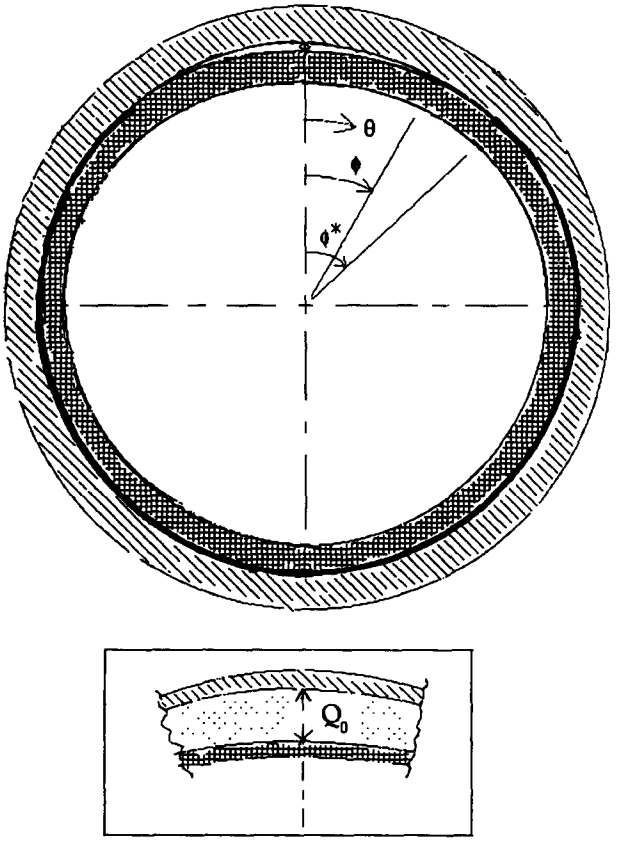

Fig. 1. Laminated cylindrical shell with delamination showing lift zone/contact zone boundary ϕ, delamination boundary ϕ^*, and self-equilibrating line load of intensity Q_0 (inset).

another. The second region will be referred to as the "contact zone" and refers to the region where the debonded segments maintain sliding contact. It is defined on the domain $S_2: \theta \in [\phi, \phi^*]$. The third region, defined on the domain $S_3: \theta \in [\phi^*, \pi]$, will be referred to as the "bond zone" and corresponds to the region where the composite cylinder remains intact or bonded. In the ensuing analysis, the undeformed interface at which the delamination occurs will be taken as the reference surface. The structure will thus be further subdivided into two sublaminates bounded by the reference surface. The inner cylinder will be referred to as sublaminate/cylinder "a", while the outer cylinder will be referred to as sublaminate/cylinder "b". In what follows, all length scales are normalized with respect to the initial radius of the reference surface. In this context we define the normalized thicknesses of the inner and outer cylinders as h_a and h_b, respectively, and define the thickness of the composite cylinder as $h^* = h_a + h_b \ll 1$.

Let us next define the normalized circumferential displacement $u_{ri}(\theta) \ll 1$ (positive clockwise) and radial displacement $w_{ri}(\theta) \ll 1$ (positive inward) of a material particle at the centerline of sublaminate r ($r = a, b$) in region i ($i = 1$–3). For the mathematical model employed, the corresponding curvature change, $\kappa_{ri}(\theta)$, and membrane strain, $e_{ri}(\theta)$, are expressed in terms of the centerline displacements as

$$\kappa_{ri} = w''_{ri} + w_{ri} \quad \text{and} \quad e_{ri} = u'_{ri} - w_{ri} + \tfrac{1}{2}w'^2_{ri}, \tag{1a, b}$$

where $f'(\theta) \equiv df/d\theta$ etc. We also define the corresponding membrane forces

$$N_{ri}(\theta) \equiv -C_r e_{ri}(\theta) \quad (r = a, b; i = 1\text{–}3), \tag{1c}$$

where C_r is the normalized membrane stiffness of cylinder r. The specific normalization of material and load parameters is discussed in Section 3. Furthermore, the circumferential displacements at the interface between cylinders a and b, u^*_{ri} ($r = a, b$), are related to those at the sublaminate centerline, u_{ri}, by

$$u^*_{bi} = u_{bi} - \tfrac{1}{2}h_b w'_{bi}, \quad u^*_{ai} = u_{ai} + \tfrac{1}{2}h_a w'_{ai}. \tag{2a, b}$$

The membrane strain in each sublaminate at the interface is similarly related to that at the corresponding centerline by

$$e_{ai} = e^*_{ai} - \tfrac{1}{2}h_a \kappa_{ai}, \quad e_{bi} = e^*_{bi} + \tfrac{1}{2}h_b \kappa_{bi} \quad (i = 1, 2, 3) \tag{3a, b}$$

where e_{ri} ($r = a, b$) corresponds to the membrane strain at the centerline and e^*_{ri} to the membrane strain in sublaminate r region i at the interface between the inner and outer sublaminates.

We next formulate an energy functional, Π, as follows;

$$\Pi = \sum_{i=1}^{3} \left\{ \sum_{r=a}^{b} U_i^{(r)} + \Lambda_i \right\} - W + \Gamma \tag{4}$$

where

$$U_i^{(r)} = \tfrac{1}{2}D_r \int_{S_i} \kappa_{ri}^2 \, d\theta + \tfrac{1}{2}C_r \int_{S_i} e_{ri}^2 \, d\theta \quad (r = a, b; i = 1\text{–}3) \tag{5a}$$

is the strain energy of sublaminate r in region i, D_r is the normalized bending stiffness of cylinder r, and the membrane strain $e_{ri}(\theta)$ is expressed in terms of the strain at the sublaminate interface and the curvature change using eqns (3a, b). The quantity Λ_i corresponds to a constraint functional associated with region i and is given by,

$$\Lambda_i = \int_{S_i} \lambda_i(w_{bi} - w_{ai})\,d\theta + \int_{S_i} \mu_i(u_{bi}^* - u_{ai}^*)\,d\theta, \tag{5b}$$

$$W = Q_0[w_{a1}(0) - w_{b1}(0)] \tag{5c}$$

represents the work done by the applied loading and

$$\Gamma = 2\gamma(\phi^* - \phi_0^*) \tag{5d}$$

is the delamination energy. In the above expressions, λ_i and μ_i ($i = 1$–3) are Lagrange multipliers with

$$\lambda_1 = 0 \quad \text{and} \quad \mu_1 = \mu_2 = 0, \tag{6a, b, c}$$

while γ is the normalized surface energy of the bond and ϕ_0^* represents an initial delamination size.

We derive the governing differential equations, boundary and matching conditions and transversality conditions upon invoking the principle of stationary potential energy. We thus require that

$$\delta\Pi = 0, \tag{7}$$

where δ corresponds to the variational operator.

Substituting eqns (1)–(6) into eqn (7), performing the proper variations and allowing for the variable boundaries at ϕ and ϕ^*, yields the governing equations, boundary conditions, matching conditions, constraint conditions and transversality conditions for the individual segments of the subcylinders a and b. Eliminating the Lagrange multipliers and employing the associated constraint conditions results in the governing equations and the boundary, matching and transversality conditions expressed in terms of the properties of the corresponding "composite structure" for $\theta \in S_2$ and $\theta \in S_3$, along with those for the individual subcylinder segments for $\theta \in S_1$. Thus we have

$$\left(D_a\kappa_{a1} + \frac{h_a}{2}N_{a1}\right)'' + \left(D_a\kappa_{a1} + \frac{h_a}{2}N_{a1}\right) + (N_{ai}w_{a1}')' + N_{a1} = 0 \quad (\theta \in S_1) \tag{8a}$$

$$\left(D_b\kappa_{b1} - \frac{h_b}{2}N_{b1}\right)'' + \left(D_b\kappa_{b1} - \frac{h_b}{2}N_{b1}\right) + (N_{b1}w_{b1}')' + N_{b1} = 0 \quad (\theta \in S_1) \tag{8b}$$

$$M_i^{*\prime\prime} + M_i^* + (N_i^* w_i^*)' + N_i^* = 0 \quad (\theta \in S_i;\ i = 2, 3) \tag{8c}$$

$$N_{ai}' = 0, \quad N_{bi}' = 0 \quad (\theta \in S_i;\ i = 1, 2) \tag{9a, b}$$

and

$$N_3^{*\prime} = 0 \quad (\theta \in S_3) \tag{9c}$$

where:

$$w_i^*(\theta) \equiv w_{ai}(\theta) = w_{bi}(\theta) \quad (\theta \in S_i;\ i = 2, 3), \tag{10a}$$

$$\kappa_i^*(\theta) \equiv \kappa_{ai}(\theta) = \kappa_{bi}(\theta) \quad (\theta \in S_i;\ i = 2, 3), \tag{10b}$$

$$u_3^*(\theta) \equiv u_{a3}^*(\theta) = u_{b3}^*(\theta) \quad (\theta \in S_3), \tag{10c}$$

$$N_2^* \equiv N_{a2} + N_{b2}, \tag{11a}$$

$$M_2^* = D_0 \kappa_2^* + m^*, \tag{11b}$$

$$m^* \equiv \left(\frac{h_a}{2} N_{a2} - \frac{h_b}{2} N_{b2} \right), \tag{11c}$$

$$M_3^* = A^* \kappa_3^* + B^* e_3^* = D^* \kappa_3^* - \rho^* N_3^*, \tag{12a}$$

$$N_3^* \equiv N_{a3} + N_{b3} = -(C^* e_3^* + B^* \kappa_3^*), \tag{12b}$$

$$A^* \equiv D_0 + (h_a/2)^2 C_a + (h_b/2)^2 C_b, \tag{13a}$$

$$B^* \equiv \tfrac{1}{2} h_b C_b - \tfrac{1}{2} h_a C_a, \tag{13b}$$

$$C^* \equiv C_a + C_b, \tag{13c}$$

$$D^* \doteq A^* - \rho^* B^* = D_0 + (h^*/2)^2 C_s, \tag{13d}$$

$$\rho^* \equiv B^*/C^*, \tag{13e}$$

$$D_0 \equiv D_a + D_b, \tag{13f}$$

and

$$C_s \equiv C_a C_b / C^*. \tag{13g}$$

The quantities A^*, B^* and C^* may be recognized as the stiffnesses of the intact composite cylinder and conform to those obtained by conventional methods. The corresponding boundary and matching conditions are then given by

$$u_{a1}(0) = w'_{a1}(0) = 0, \quad [D_a \kappa'_{a1} + N_{a1} w'_{a1}]_{\theta=0} = Q_0, \tag{14a, b, c}$$

$$u_{b1}(0) = w'_{b1}(0) = 0, \quad [D_b \kappa'_{b1} + N_{b1} w'_{b1}]_{\theta=0} = -Q_0, \tag{14d, e, f}$$

$$u_{a1}^*(\phi) = u_{a2}^*(\phi), \qquad u_{b1}^*(\phi) = u_{b2}^*(\phi), \tag{15a, b}$$

$$N_{a1}(\phi) = N_{a2}(\phi), \qquad N_{b1}(\phi) = N_{b2}(\phi), \tag{15c, d}$$

$$w_{a1}(\phi) = w_{b1}(\phi) = w_2^*(\phi), \tag{15e, f}$$

$$w'_{a1}(\phi) = w'_{b1}(\phi) = w_2^{*\prime}(\phi), \tag{15g, h}$$

$$\left[D_a \kappa_{a1} + \frac{h_a}{2} N_{a1} \right]_{\theta=\phi} + \left[D_b \kappa_{b1} - \frac{h_b}{2} N_{b1} \right]_{\theta=\phi} = [D_0 \kappa_2^* + m^*]_{\theta=\phi}, \tag{15i}$$

$$\left[D_a \kappa'_{a1} + \frac{h_a}{2} N'_{a1} + N_{a1} w'_{a1} \right]_{\theta=\phi} + \left[D_b \kappa'_{b1} - \frac{h_b}{2} N'_{b1} + N_{b1} w'_{b1} \right]_{\theta=\phi} = [D_0 \kappa_2^{*\prime} + m^{*\prime} + N_2^* w_2^{*\prime}]_{\theta=\phi}, \tag{15j}$$

$$u_{2a}^*(\phi^*) = u_{2b}^*(\phi^*) = u_3^*(\phi^*), \qquad N_2^*(\phi^*) = N_3^*(\phi^*), \tag{16a, b, c}$$

$$w_2^*(\phi^*) = w_3^*(\phi^*), \qquad w_2^{*\prime}(\phi^*) = w_3^{*\prime}(\phi^*), \tag{16d, e}$$

$$M_2^*(\phi^*) = M_3^*(\phi^*), \quad [M_2^{*\prime} + N_2^* w_2^{*\prime}]_{\theta=\phi^*} = [M_3^{*\prime} + N_3^* w_3^{*\prime}]_{\theta=\phi^*}, \tag{16f, g}$$

$$u_3^*(\pi) = w_3^{*\prime}(\pi) = 0, \quad [M_3^{*\prime} + N_3^* w_3^{*\prime}]_{\theta=\pi} = 0. \tag{17a, b, c}$$

In addition, the transversality conditions found as a result of the variable boundaries at $\theta = \phi$ and $\theta = \phi^*$ take the form of

$$\kappa_{a1}(\phi) = \kappa_{b1}(\phi) = \kappa_2^*(\phi), \tag{18}$$

which defines the equilibrium configurations of the propagating boundary between the contact zone and the zone of separation, and

$$G_a\{\phi^*\} \equiv \left[\frac{1}{2}D_0\kappa_2^{*2} + \frac{1}{2C_a}N_a^2 + \frac{1}{2C_b}N_b^2\right]_{\theta=\phi^*} - \left[\frac{1}{2}D^*\kappa_3^{*2} + \frac{1}{2C^*}N_3^{*2}\right]_{\theta=\phi^*} = 2\gamma \quad (\phi \leqslant \phi^{*-}), \tag{19a}$$

$$G_b\{\phi^*\} \equiv \left[\frac{1}{2}D_a\kappa_{a1}^2 + \frac{1}{2}D_b\kappa_{b1}^2 + \frac{1}{2C_a}N_a^2 + \frac{1}{2C_b}N_b^2\right]_{\theta=\phi^*} - \left[\frac{1}{2}D^*\kappa_3^{*2} + \frac{1}{2C^*}N_3^{*2}\right]_{\theta=\phi^*} = 2\gamma(\phi = \phi^*), \tag{19b}$$

which define the equilibrium configurations of the propagating boundary of the delamination. The quantities G_a and G_b may be identified as the energy release rates at the delamination edge.

The transversality conditions which define the boundary $\theta = \phi^*$ suggest the following growth criterion: if for an initial delamination boundary $\phi^* = \phi_0^*$,

$$G_a\{\phi_0^*\} < 2\gamma \quad (\phi \leqslant \phi^{*-}),$$
$$G_b\{\phi_0^*\} < 2\gamma \quad (\phi = \phi^*),$$

no growth occurs and ϕ^* remains at its initial value; if for an initial delamination boundary $\phi^* = \phi_0^*$,

$$G_a\{\phi_0^*\} > 2\gamma \quad (\phi \leqslant \phi^{*-}),$$
$$G_b\{\phi_0^*\} > 2\gamma \quad (\phi = \phi^*),$$

growth occurs, with the system evolving such that the equality (19) is satisfied. The energy release G_a is seen to correspond to mode II fracture, while the energy release G_b is seen to correspond to a combination of mode I and mode II fracture. The growth criterion following eqns (19a, b) is interpreted accordingly.

The problem of interest is fully defined at this point. It can, however, be put into a more convenient form by recasting it into a mixed formulation expressed in terms of the radial displacements and the membrane forces. Upon integrating eqns (9a–c), noting eqn (11a) and imposing the matching conditions [eqns (15c, d) and eqn (16c)], we find that

$$N_{a1} = N_{a2} = N_{a0} = \text{constant}, \tag{20a}$$
$$N_{b1} = N_{b2} = N_{b0} = \text{constant}, \tag{20b}$$
$$N_2^* = N_3^* = N^* = \text{constant}\,(= N_{a0} + N_{b0}). \tag{20c}$$

Substitution of eqns (20a–c) into eqn (11c) yields

$$m^* = m_a + m_b = \text{constant}, \tag{20d}$$

where

$$m_a \equiv N_{a0}h_a/2 \quad \text{and} \quad m_b \equiv -N_{b0}h_b/2. \tag{21a, b}$$

On incorporating eqns (20a–c) into eqns (8a–d), the governing differential equations take the forms

$$L\{w_r; N_{r0}/D_r\} + (m_r/D_r) = 0 \quad (r = a, b), \tag{22a, b}$$

$$L\{w_2^*; N^*/D_0\} + (m^*/D_0) = 0 \tag{22c}$$

and

$$L\{w_3^*; N^*/D^*\} - (\rho^* N^*/D^*) = 0, \tag{22d}$$

where

$$L\{w; N\} \equiv \frac{d^4 w}{d\theta^4} + (2+N)\frac{d^2 w}{d\theta^2} + w + N. \tag{23}$$

The quantities m_a, m_b, m^* and $\rho^* N^*$ are seen to be the moments of the membrane forces of the respective cylindrical segments, taken about the reference surface.

Upon substituting eqns (20a, b) into eqn (1c), eqn (20c) into eqn (12b), integrating over the corresponding domain and applying the boundary conditions of eqns (14a, d) and (15a, b) for $\theta \in S_1 + S_2$, and eqns (16a, b) with eqn (17a) for $\theta \in S_3$, we obtain the circumferential displacements of the corresponding cylindrical segments at $\theta = \phi^*$ in terms of the radial displacements and the membrane forces. Thus,

$$u_{a2}^*(\phi^*) = U_a^* \equiv -\frac{N_{a0}}{C_a}\phi^* + \frac{h_a}{2}w_2^{*\prime}(\phi^*) + \int_0^{\phi} (w_{a1} - \tfrac{1}{2}w_{a1}'^2)\, d\theta + \int_{\phi}^{\phi^*} (w_2^* - \tfrac{1}{2}w_2^{*\prime 2})\, d\theta, \tag{24a}$$

$$u_{b2}^*(\phi^*) = U_b^* \equiv -\frac{N_{b0}}{C_b}\phi^* - \frac{h_b}{2}w_2^{*\prime}(\phi^*) + \int_0^{\phi} (w_{b1} - \tfrac{1}{2}w_{b1}'^2)\, d\theta + \int_{\phi}^{\phi^*} (w_2^* - \tfrac{1}{2}w_2^{*\prime 2})\, d\theta \tag{24b}$$

and

$$u_3^*(\phi^*) = U_3^* \equiv \frac{N^*}{C^*}(\pi - \phi^*) - \rho^* w_3^{*\prime}(\phi^*) - \int_{\phi^*}^{\pi} \{(1-\rho^*)w_3^* - \tfrac{1}{2}w_3^{*\prime 2}\}\, d\theta. \tag{24c}$$

Each of the above expressions (24a–c) may be equated by virtue of the matching conditions (16a, b). Doing so results in a pair of "integrability conditions" in terms of the radial displacements and the membrane forces, the load intensity Q_0, and the boundary angles ϕ and ϕ^* of the form

$$I_j\{w_{a1}, w_{b1}, w_2^*, w_3^*; N_{a0}N_{b0}, N^*; Q_0; \phi, \phi^*\} = 0 \quad (j = 1, 2) \tag{25}$$

where, for example,

$$I_1 = I_a \equiv U_a^* - U_3^* = 0 \tag{25a}$$

and

$$I_2 = I_b \equiv U_b^* - U_3^* = 0. \tag{25b}$$

This explicitly eliminates the circumferential displacements from the formulation.

The differential eqns (22a–d) together with the integrability conditions, the transversality conditions and the remaining boundary and matching conditions, recast the mathematical problem from a displacement formulation (expressed in terms of both the radial displacements and the circumferential displacements) to a mixed formulation (expressed in terms of the radial displacements and the membrane forces).

3. ANALYTICAL SOLUTION

We next present a solution to the problem in hand posed in the mixed formulation given at the end of the previous section. In all that follows, the normalized sublaminate stiffnesses are given by

$$C_a = 12/h_a^2, \quad D_a = 1, \quad C_b = C_a/E_0 h_0, \quad D_b = 1/E_0 h_0^3, \tag{26a–d}$$

where

$$h_0 = h_a/h_b, \quad E_0 = \frac{E_a/(1-\nu_a^2)}{E_b/(1-\nu_b^2)} \quad \text{or} \quad E_0 = E_a/E_b \tag{26e, f}$$

and E_r and ν_r ($r = a, b$) correspond to Young's modulus and Poisson's ratio of the inner and outer sublaminates, respectively. In a similar fashion, the normalized load intensity Q_0 is related to its dimensional counterpart $\bar{Q}$ and the normalized bond energy γ is related to its dimensional counterpart $\bar{\gamma}$ by $\gamma = \bar{\gamma}R^2/\bar{D}$ and $Q_0 = \bar{Q}R^2/\bar{D}$, respectively, where R is the initial radius of the reference surface and $\bar{D}$ is the dimensional bending stiffness of the inner sublaminate.

Before proceeding formally we first note, upon consideration of a free body diagram of a portion of the composite structure, that for the loading type considered, the total membrane force N^* vanishes throughout the structure. Further consideration shows that the total shear on any cross section vanishes as well, while the total internal moment is, at most, uniform. That is to say that the internal moment of the composite structure does not vary with θ. Consideration of eqn (8c) indicates that for $N^* = 0$, the only admissible uniform moments for the present model of the composite cylinder are those that vanish.

It is thus seen, from eqns (12a, b) that $\kappa_3^* = e_3^* = 0$ and hence that the laminated segment is undeformed (i.e. for the present laminate model, the portion of the structure on $[\phi, \phi^*]$ is impervious to the "stress" distribution, the resultant of which vanishes, imposed on it at $\theta = \phi^*$ and hence responds rigidly). It is further seen from eqn (11b), that the curvature of the composite structure, and hence of the sublaminates as well, is uniform throughout the contact zone.

From the above discussion we may deduce the following;

$$N^* = 0 \quad \text{hence} \quad N_{b0} = -N_{a0} = -N_0 \quad (\theta \in S_1 + S_2), \tag{27a}$$

$$\kappa_2^*(\theta) = -\kappa_0 \equiv -m^*/D_0 = -N_0 h^*/2D_0 \quad (\theta \in S_2) \tag{27b}$$

and

$$N^* = u_3^*(\theta) = w_3^*(\theta) = 0 \quad (\theta \in S_3) \tag{28a, b, c}$$

where for definiteness, we have restricted the system from rigid body translation by introducing, say, a knife edge at the base of the system. The relationship (27a) now replaces one of the integrability conditions, say eqn (25b), as N_{b0} is now known in terms of N_{a0} explicitly. The differential eqns (22a–c), together with the corresponding boundary and matching conditions, then lead to the following solutions for the radial deflections of the individual shell segments for $\theta \in S_1 + S_2$, as functions of the load intensity Q_0, the membrane force N_0, the lift zone/contact zone boundary angle ϕ and the delamination boundary angle ϕ^*;

$$w_{a1}(\theta) = \{Q_0 q_a + p_a\} \cos \alpha\theta - \{Q_0 v_a + t_a\} \cos \theta/\alpha - Q_0 F_a(\theta; \alpha) - N_0(1 + h_a/2), \tag{29a}$$

$$w_{b1}(\theta) = \{Q^* q_b + p_b\} f(\theta; P_0) - \{Q^* v_b + t_b\} g(\theta; P_0) - Q^* F_b(\theta; P_0) + P_0(1 - h_b/2), \tag{29b}$$

$$w_2^*(\theta) = -\kappa_0 F^*(\theta; \phi^*) \tag{29c}$$

where the functions F_a and F^* are given by

$$F_a(\theta;\alpha) = \frac{\alpha}{\alpha^4-1}(\sin\alpha\theta - \alpha^2\sin\theta/\alpha) \tag{30}$$

and

$$F^*(\theta;\phi^*) = 1-\cos\phi^*\cos\theta - \sin\phi^*\sin\theta \tag{31}$$

and the parameter α is related to the normalized membrane force N_0, by

$$\alpha^2 = \tfrac{1}{2}[N_0+2+\sqrt{N_0(N_0+4)}] > 1 \quad \text{or} \quad N_0 = (\alpha^2-1)^2/\alpha^2. \tag{32}$$

In addition, the functions that describe the deflection of the outer shell for $\theta \in S_1$ are dependent upon the parameters

$$P_0 = N_0/D_b \quad \text{and} \quad Q^* = Q_0/D_b \tag{33a, b}$$

and are given by

(i) $P_0 < 4$;

$$f(\theta;P_0) = \cosh\xi\theta\cos\eta\theta, \tag{34a}$$

$$g(\theta;P_0) = \sinh\xi\theta\sin\eta\theta, \tag{34b}$$

$$F_b(\theta;P_0) = \tfrac{1}{2}e^{\xi\theta}\left[\frac{\sin\eta\theta}{\eta} - \frac{\cos\eta\theta}{\xi}\right] \tag{34c}$$

where

$$\eta = \cos\chi, \quad \xi = \sin\chi, \tag{35a, b}$$

$$\chi = 2\tan^{-1}\left\{\frac{\sqrt{P_0(4-P_0)}}{2-P_0}\right\} \quad (P_0 \neq 2), \tag{36a}$$

$$\chi = \pi/4 \quad (P_0 = 2), \tag{36b}$$

or by

(ii) $P_0 > 4$;

$$f(\theta;P_0) = \cosh\beta\theta, \tag{37a}$$

$$g(\theta;P_0) = \cosh\theta/\beta, \tag{37b}$$

$$F_b(\theta;P_0) = \frac{\beta}{\beta^4-1}(\sinh\beta\theta - \beta^2\sinh\theta/\beta), \tag{37c}$$

where the parameter β is related to the membrane force parameter P_0 by

$$\beta^2 = \tfrac{1}{2}[P_0-2+\sqrt{P_0(P_0-4)}]. \tag{38}$$

The coefficients appearing in eqn (29a) are given by

$$q_a = q_a(\alpha, \phi) = [F_a^{(0)} \sin \phi/\alpha + F_a^{(1)} \alpha \cos \phi/\alpha]/X_a, \tag{39a}$$

$$p_a = p_a(\alpha, \phi, \phi^*) = [P^* \sin \phi/\alpha - \kappa_0 F^{*(1)} \alpha \cos \phi/\alpha]/X_a, \tag{39b}$$

$$v_a = v_a(\alpha, \phi) = [F_a^{(0)} \alpha \sin \alpha\phi + F_a^{(1)} \cos \alpha\phi]\alpha/X_a \tag{39c}$$

and

$$t_a = t_a(\alpha, \phi, \phi^*) = [P^* \alpha \sin \alpha\phi - \kappa_0 F^{*(1)} \cos \alpha\phi]\alpha/X_a, \tag{39d}$$

where

$$X_a = X_a(\alpha, \phi) = \cos \alpha\phi \sin \phi/\alpha - \alpha^2 \sin \alpha\phi \cos \phi/\alpha, \tag{40a}$$

$$P^* = P^*(\alpha, \phi, \phi^*) = N_0(1 + h_a/2) - \kappa_0 F^{*(0)}, \tag{40b}$$

and we have introduced the notation

$$f^{(n)} \equiv \left.\frac{d^n f}{d\theta^n}\right|_{\theta=\phi} \tag{41}$$

for any function $f(\theta)$.

The coefficients appearing in eqn (29b) are similarly given by

$$q_b = q_b(P_0, \phi) = [F_b^{(0)} g^{(1)} - F_b^{(1)} g^{(0)}]/X_b, \tag{42a}$$

$$p_b = p_b(P_0, \phi, \phi^*) = [\kappa_0(\omega_0 g^{(1)} - \omega_1 g^{(0)}) - P^* g^{(1)}]/X_b, \tag{42b}$$

$$v_b = v_b(P_0, \phi) = [F_b^{(0)} f^{(1)} - F_b^{(1)} f^{(0)}]/Y_b \tag{42c}$$

and

$$t_b = t_b(P_0, \phi, \phi^*) = [\kappa_0(\omega_0 f^{(1)} - \omega_1 f^{(0)}) - P^* f^{(1)}]/Y_b, \tag{42d}$$

where

$$X_b = X_b(P_0, \phi) = g^{(0)} f^{(1)} - g^{(1)} f^{(0)}, \tag{43a}$$

$$Y_b = Y_b(P_0, \phi) = f^{(0)} g^{(1)} - f^{(1)} g^{(0)}, \tag{43b}$$

$$\omega_0 = \omega_0(\phi, \phi^*) = \cos \phi^* \cos \phi + \sin \phi^* \sin \phi - 1 \tag{43c}$$

and

$$\omega_1 = \omega_1(\phi, \phi^*) = \sin \phi^* \cos \phi - \cos \phi^* \sin \phi. \tag{43d}$$

Substitution of the above solutions for the radial deflections (29a, c) along with eqn (28) into the integrability condition (25a) transforms that condition into a nonlinear algebraic equation which defines the membrane forces associated with equilibrium configurations of the evolving system. We thus have

$$\{Q_0 q_a + p_a\} \frac{\sin \alpha\phi}{\alpha} - \{Q_0 v_a + t_a\} \alpha \sin \phi/\alpha + Q_0 \left[\frac{\cos \alpha\phi - \alpha^4 \cos \phi/\alpha}{\alpha^4 - 1}\right]$$

$$- \frac{1}{2}\left\{\frac{\alpha}{4}\{Q_0 q_a + p_a\}^2 [\Omega_1 - \sin \Omega_1] + \frac{\{Q_0 v_a + t_a\}^2}{4\alpha} [\Omega_2 - \sin \Omega_2]\right.$$

$$-\{Q_0q_a+p_a\}\{Q_0v_a+t_a\}\phi\left[\frac{\sin\psi_1}{\psi_1}-\frac{\sin\psi_2}{\psi_2}\right]$$

$$+Q_0^2\frac{\alpha^4\phi}{(\alpha^4-1)^2}\left[1+\frac{\sin\Omega_1}{2\Omega_1}+\frac{\sin\Omega_2}{2\Omega_2}-\frac{\sin\psi_1}{\psi_1}-\frac{\sin\psi_2}{\psi_2}\right]$$

$$+Q_0\{Q_0q_a+p_a\}\frac{\alpha^3\phi}{\alpha^4-1}\left[\frac{\sin^2\alpha\phi}{\alpha\phi}+\frac{\cos\psi_2}{\psi_2}+\frac{\cos\psi_1}{\psi_1}-\frac{2\alpha^3}{(\alpha^4-1)\phi}\right]$$

$$+Q_0\{Q_0v_a+t_a\}\frac{\alpha\phi}{\alpha^4-1}\left[\frac{\sin^2\phi/\alpha}{\phi/\alpha}+\frac{\cos\psi_2}{\psi_2}-\frac{\cos\psi_1}{\psi_1}+\frac{2\alpha}{(\alpha^4-1)\phi}\right]\Bigg\}$$

$$-N_0\{\phi(1+h_a/2)+\phi^*/C_a\}-\kappa_0\{\phi^*-\phi+\cos\phi^*\sin\phi-\sin\phi^*\cos\phi\}$$

$$-\frac{\kappa_0^2}{4}\{(\phi^*-\phi)+(\sin^2\phi^*-\cos^2\phi^*)(\cos\phi^*\sin\phi^*-\cos\phi\sin\phi)$$

$$-2\cos\phi^*\sin\phi^*(\sin^2\phi^*-\sin^2\phi)\}=0 \tag{44}$$

where

$$\Omega_1=2\alpha\phi,\quad \Omega_2=2\phi\alpha, \tag{45a, b}$$

$$\psi_1=\frac{\alpha^2-1}{\alpha}\phi\quad\text{and}\quad\psi_2=\frac{\alpha^2+1}{\alpha}\phi. \tag{45c, d}$$

Substitution of eqns (29a, c) into eqn (18) transforms the transversality condition at the lift zone/contact zone boundary to the form

$$\{\kappa_0F^{*(2)}-p_a\alpha^2\cos\alpha\phi+t_a\cos\phi/\alpha\}-Q_0\{q_a\alpha^2\cos\alpha\phi-v_a\cos\phi/\alpha+F_a^{(2)}\}=0(\phi\leqslant\phi^{*-}). \tag{46}$$

Substitution of the solutions (27a) and (28a, c) together with the solution (29c) into the transversality condition at the delamination boundary (19a) while incorporating the matching condition (16f), reduces the growth equation to the form

$$G_a\{\phi^*\}=G_{II}\equiv\frac{1}{2D_0}m^{*2}+\frac{1}{2C_s}N_0^2=2\gamma\quad(\phi\leqslant\phi^{*-}). \tag{47a}$$

Similar substitutions incorporating the solutions (27a), (28a, c) and (29a), while accounting for the moment balance at the delamination edge for the case where the lift zone completely envelops the contact zone, renders the transversality condition (19b) to the equivalent form

$$\{-\kappa^*-p_a\alpha^2\cos\alpha\phi^*+t_a\cos\phi^*/\alpha\}-Q_0\{q_a\alpha^2\cos\alpha\phi^*-v_a\cos\phi^*/\alpha+F_a^{(2)}\}=0(\phi=\phi^*) \tag{47b}$$

where

$$\kappa^*\equiv\kappa_{a1}(\phi^*)=-\kappa_0+\sqrt{2(2\gamma-G_{II})}. \tag{48}$$

In eqn (48), the positive root is taken so as to render the curvature difference $[\kappa_{a1}-\kappa_{b1}]_{\theta=\phi^*}\geqslant 0$ and thus correspond to a physically realizable state of the system. The limiting case, $\kappa^*=-\kappa_0$ corresponds to the situation where the lift zone just traverses the entire delamination (i.e. when $\phi=\phi^{*-}$). In such a situation the conditions (46) and (47a) are satisfied as well.

Equation (44) together with eqns (46) and (47a) or together with eqn (47b) constitute two systems of coupled nonlinear algebraic equations, one for $\phi\leqslant\phi^{*-}$ and the other for $\phi=\phi^*$, in terms of the membrane force N_0, the lift zone/contact zone boundary angle ϕ,

the delamination boundary angle ϕ^* and the load intensity Q_0. Quadruples $\{N_0, \phi, \phi^*, Q_0\}$ which satisfy the system of algebraic equations correspond to equilibrium configurations of the delaminating structure.

It is seen that, as a result of the rigid body response of the intact composite structure ($\theta \in [\phi^*, \pi]$), only the solution of the inner (outer) cylinder for $\theta \in [0, \phi]$ [eqn (29a or b)], along with that of the composite cylinder for $\theta \in [\phi, \phi^*]$ [eqn (29c)], is explicitly needed to evaluate the propagation characteristics of the boundaries $\theta = \phi$ and $\theta = \phi^*$ given the material properties of both the inner and outer sublaminates and of the bond. Such characteristics of the evolving structure are examined in the next section.

4. NUMERICAL RESULTS AND DISCUSSION

In the present section we shall examine the characteristics of the evolving structure by considering variations of a specific system. As is indicated by the theory and analysis presented to this point, the phenomenon of delamination growth, in the present context, is dependent upon the relative stiffnesses of the two sublaminates, as well as on the bond strength, for a given loading program. As seen by equations (26a–f), the relative stiffnesses are dependent upon the ratio of the material parameters (Young's modulus, Poisson's ratio) of the pair of subcylinders and on their relative thicknesses. For the purposes of comparison, we shall vary the material ratio E_0 for a structure whose inner and outer sublaminates are of equal thickness. This will be done for the specific system whose normalized sublaminate thicknesses are $h_a = h_b = 0.002449$.

As discussed previously, growth of the delamination may occur when the debonded region possesses a contact zone or when the lift zone traverses the entire delamination. For the former, the lift zone/contact zone boundary propagates (recedes) as well. We shall consider the case of nonvanishing contact zone first.

When $\phi \leqslant \phi^{*-}$, substitution of eqn (46) into eqn (44) eliminates the load parameter Q_0 resulting in a nonlinear algebraic equation in α (N_0), ϕ and ϕ^*. Thus for a given delamination size ϕ^*, the resulting equation may be solved numerically to obtain values of the membrane force parameter α, for selected values of the lift zone/contact zone boundary angle ϕ. This is done numerically via the bisection technique. The resulting roots may then be substituted into eqns (46) and (47a) to obtain the corresponding values of the load intensity Q_0 and the energy release rate G_a, respectively. Selected results are displayed in Figs 2–4 in the form of plots of Q_0 vs G_a.

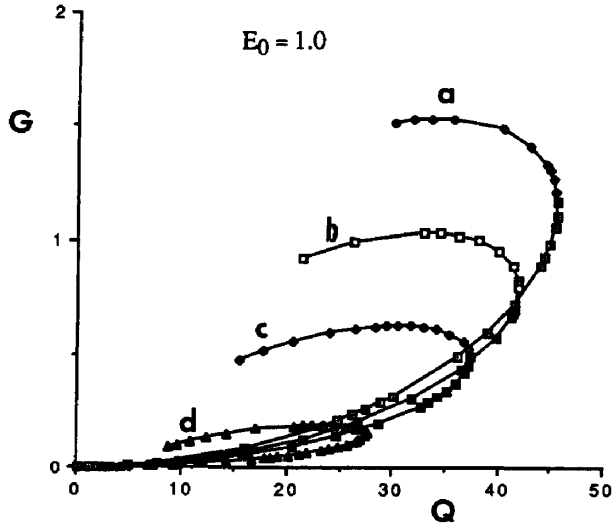

Fig. 2. Energy release rate vs load intensity for various delamination sizes, for the case of finite contact zone with $E_0 = 1.0$; (a) $\phi^* = 0.15$, (b) $\phi^* = 0.17$, (c) $\phi^* = 0.20$, (d) $\phi^* = 0.30$. ($h_a = h_b = 0.002449$).

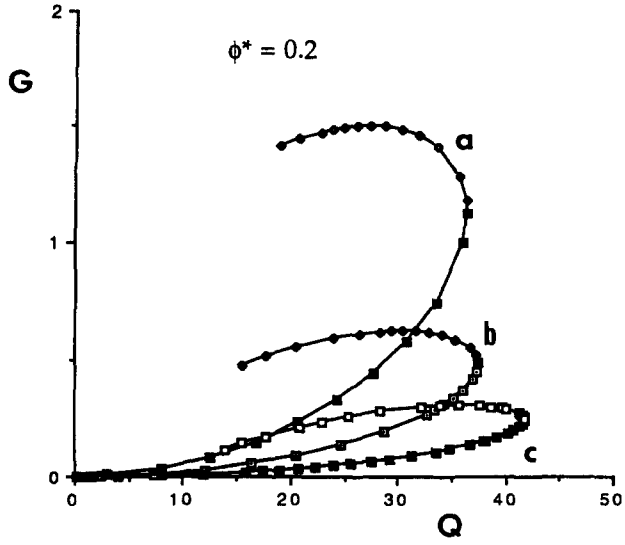

Fig. 3. Comparison of energy release rate vs load intensity for $\phi^* = 0.20$ for various values of moduli ratios for the case of finite contact zone; (a) $E_0 = 10.0$, (b) $E_0 = 1.0$, (c) $E_0 = 0.10$. ($h_a = h_b = 0.002449$).

The behavior of a selected set of delaminations with nonvanishing contact zone is illustrated in Fig. 2 for the case where $E_0 = 1$, while the effect of variation of the modulus ratio and hence of the relative stiffnesses of the subcylinders is demonstrated in Fig. 3 for a delamination size of $\phi^* \simeq 0.2$. Upon examination of Fig. 2, it may first be noted that the overall relative features of the corresponding curves resemble those of the (inner) thin film case (Bottega, 1988b) in a qualitative sense. For each curve, corresponding to a different delamination length, the energy release rate increases monotonically with increasing load intensity until a maximum value of $Q_0 = Q_{cr}$ is achieved. This load corresponds to the critical load at which snap-through buckling occurs. As we proceed around the remainder of the curve, the energy release rate further increases before decreasing, with decreasing load intensity. For each of these paths, the lift zone/bond zone boundary angle first decreases then increases, as each of the curves is traversed in a counter-clockwise manner. The curves terminate at the point where $\phi = \phi^*$. Thus, for $Q_0 \to 0^+$ an initial value of ϕ is achieved.

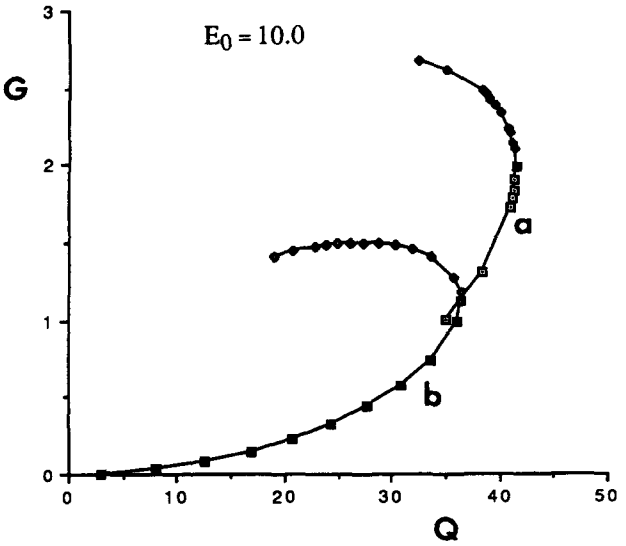

Fig. 4. Energy release rate vs load intensity for $E_0 = 10.0$ for the case of finite contact zone; (a) $\phi^* = 0.17$, (b) $\phi^* = 0.20$. ($h_a = h_b = 0.002449$).

Further, solutions for non-vanishing contact zone cease to exist for delamination sizes below a certain value, that is, roots could not be found for these cases. In this particular case ($E_0 = 1$) the minimum delamination size with non-vanishing contact zone is approximately $\phi^* \approx 0.14^-$. This characteristic is consistent with what was observed for the thin film case (Bottega, 1988b) but occurs at slightly larger values of the minimum delamination angle (0.14 for $E_0 = 1.0$ and 0.17 for $E_0 = 10.0$, compared with 0.10 for the thin film case) due to the added flexibility of the present system. A reason for this minimum value is that as $\phi^* \to O(h^+)$, the "arch" tends to a flat layer and the behavior then acts in kind (i.e. no contact zone) under load. This also suggests a rationale for the finite value of the lift zone boundary ϕ for $Q_0 \to 0^+$. Alternatively, for a large enough disbond, the initial deformation of the sublaminates is primarily membrane in nature upon application of the load, hence the initial separation angle (non-vanishing ϕ). Such behavior is demonstrated for the case of concentric rings (Bottega, 1993). Further increases in load result in a combination of bending of the composite structure in the contact zone and bending of the individual segments in the separation zone, in addition to stretching (compressing) of the segments, such that ϕ first decreases and then increases. It may be noted that the curves in Fig. 2 become closer to one another (i.e. more densely packed) as ϕ^* increases, and that the curves intersect one another at a single point for each pair. If we consider some initial delamination size, the corresponding curve would be traversed (for $Q_0 < Q_{cr}$) until $G_a = 2\gamma$ at which point growth will occur. When growth does occur, the figure indicates that increments in the load will cause incremental increases in the delamination size. Such stable growth will continue to occur (with increasing "rate") as the load is increased, until a path corresponding to a delamination size is encountered such that the maximum load of that path is intercepted for the given value of the critical energy release rate. If γ is large enough, such a point will be achieved without growth. At this point snap-through occurs and $\phi \to \phi^*$. Growth is then governed by eqn (47b) and is discussed later in this section. It may be pointed out that although points of intersection occur between paths of different size delaminations, the states associated with the larger disbonds are not directly achievable from those of the smaller at constant Q_0. This may be seen if one observes, for example, the paths shown in Fig. 2 for $Q_0 \approx 37$. From the variation in energy levels as a function of delamination size one can infer that a relative minimum in the energy release rate occurs between $\phi^* = 0.17$ and $\phi^* = 0.20$, and thus that an "energy barrier" exists between these two disbond sizes at this load level.†

It is seen from Fig. 3 that, as the modulus ratio is increased (for fixed values of the stiffness parameters of the inner cylinder), the energy release rate increases accordingly while the corresponding maximum load decreases as the overall structure becomes more compliant in the context of the type of loading considered. The corresponding curve for the thin film case ($E_0 \to 0$; Bottega, 1988b) differs slightly from the case for $E_0 = 0.1$ shown. It is also interesting to note that for the case where $E_0 = 10.0$, the minimum delamination size at which a contact zone is found is $\phi^* \approx 0.17$. For $\phi^* = 0.17$, the initial and terminating lift zone boundary is at $\phi = \phi^* = 0.17$ (Fig. 4). Thus, such a state may not, in general, be achievable from initial loading but may be approached after growth of a smaller disbond with vanishing contact zone. Alternatively, the layers may separate throughout the debonded region upon initial loading and first come into contact when $Q_0 = 35$. If the initial delamination size is smaller than the minimum required for a contact zone to exist, or if $\phi < \phi^*$ and snap-through buckling occurs with $\phi \to \phi^*$ as discussed, growth is governed by eqn (47b). Eliminating Q_0 from eqns (47b) and (44) results in a single nonlinear algebraic equation which may be solved numerically for given ϕ^*, as for the previous case, to yield values of N_0 corresponding to equilibrium configurations of the delaminating structure. These values may then be substituted into eqn (47b) to yield the corresponding

† It should be pointed out here that the opposite was stated for the analogous problem with a rigid outer cylinder [Bottega (1988b) and the corresponding paragraph in the review, Bottega (1988d)] where the intersection points for paths corresponding to $\phi < \phi^*$ were said to indicate unstable growth. We take this opportunity to correct that statement and thus to indicate that the scenario for $\phi < \phi^*$ for the analogous rigid substrate problem should parallel the discussion for the more general case considered herein.

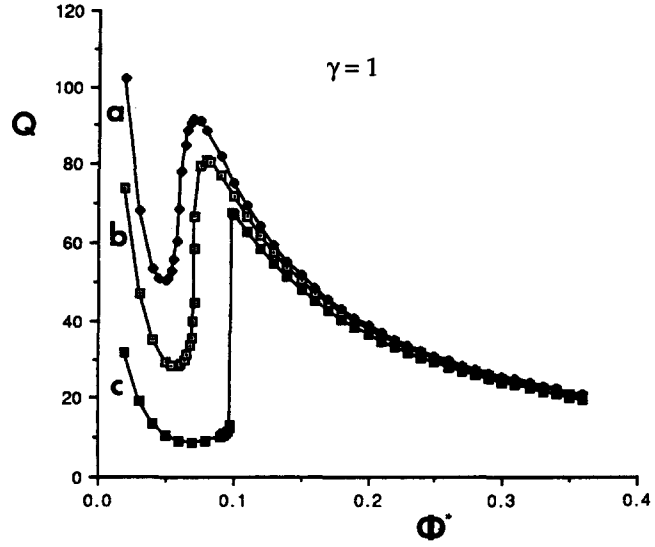

Fig. 5. Delamination growth paths for the case of vanishing contact zone with $\gamma = 1.0$ for various moduli ratios; (a) $E_0 = 0.10$, (b) $E_0 = 1.0$, (c) $E_0 = 10.0$. ($h_a = h_b = 0.002449$).

values of Q_0. The delamination growth paths for $E_0 = 0.1$, 1.0 and 10.0, are displayed in Figs 5 and 6 for bond strengths of $\gamma = 1.0$ and $\gamma = 10.0$, respectively.

Upon observation of Figs 5 and 6 it is seen that each path, in general, possesses an "unstable well" and that this well deepens and widens with increasing modulus ratio and decreasing bond strength. It is also observed that two critical points, ϕ_{c2}^* and ϕ_{c1}^*, exist corresponding to the peak at the right hand boundary of the well and its projection onto the left hand boundary of the well, respectively (see Fig. 7). When growth occurs for delaminations whose initial size is $\phi_0^* < \phi_{c1}^*$ or $\phi_0^* > \phi_{c2}^*$ for the system in question, it is unstable and catastrophic within the context of the present model. A second critical point, ϕ_b^*, exists corresponding to the bottom most point of each well (see Fig. 7). When growth occurs for disbonds whose sizes are bounded by the critical points for catastrophic growth and lie to the left of the bottom of the well, i.e. when $\phi_{c1}^* < \phi_0^* < \phi_b^*$, growth is unstable. When growth occurs for disbonds whose sizes are bounded by the critical points for

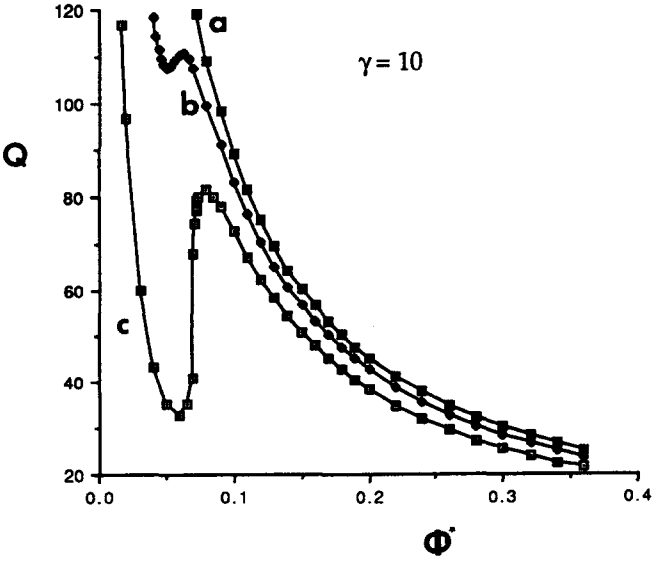

Fig. 6. Delamination growth paths for the case of vanishing contact zone with $\gamma = 10.0$ for various moduli ratios; (a) $E_0 = 0.10$, (b) $E_0 = 1.0$, (c) $E_0 = 10.0$. ($h_a = h_b = 0.002449$).

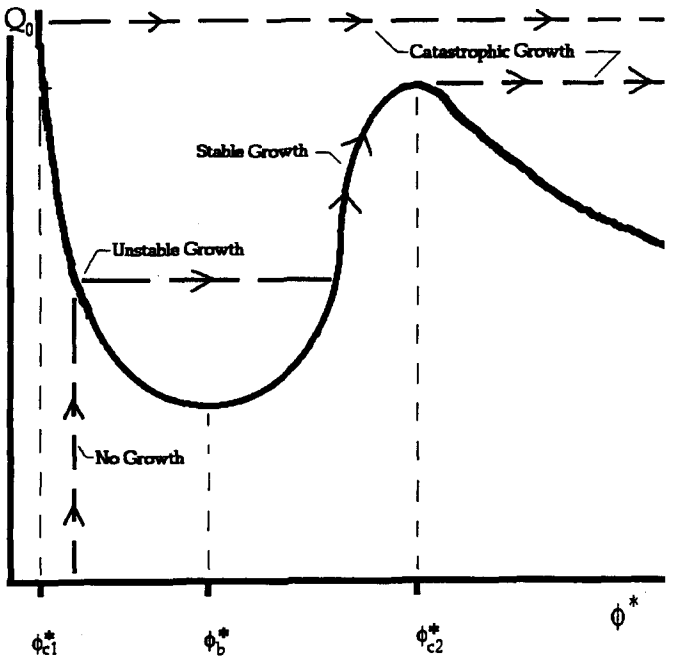

Fig. 7. Generic delamination growth path for the case of vanishing contact zone, showing critical delamination sizes ϕ^*_b, ϕ^*_{c1} and ϕ^*_{c2}, separating regions of stable, unstable and catastrophic growth (representative scenarios are depicted).

catastrophic growth and lie to the right of the bottom of the well, i.e. when $\phi^*_b \leqslant \phi^*_0 < \phi^*_{c2}$, growth is stable. For the case where $E_0 = 10.0$ and $\gamma = 1.0$, the ascending portion of the well is actually of a very narrow "S" shape, not seen within the resolution of the figure. Such a shape indicates minor closure at this point or, if one does not allow closure, arrest until the peak is encountered. In any case, the ascending (right hand) portion of each well indicates stable growth for all other cases considered. For the case of a very weak bond, $\gamma = 0.1$ (not shown), the growth paths for vanishing contact zone terminate after they encounter the stable (right hand) portion of the wells for the range of values considered. At these points $G_{II} \to 2\gamma$ and thus $\kappa^* \to \kappa_0$. These points correspond to the limiting case of vanishing/nonvanishing contact zone, where the lift zone just traverses the delamination. Such results indicate that for situations in which this occurs, the propagating delamination develops contact zones for delaminations which grow beyond these limiting sizes and is reminiscent of the behavior observed for a thin layer debonding from a contracting cylinder (Bottega, 1988a, c). This behavior suggests how a delamination which possesses a non-vanishing contact zone but does not possess equilibrium configurations which are achievable by loading from the undeformed state, such as that represented by the curve shown in Fig. 4 corresponding to $\phi^* = 0.17$ (and discussed earlier), may be encountered.

For a disbond whose initial size is such that no contact zone exists, a typical scenario would be the following; as the applied load intensity Q_0 is increased from zero, the sublaminates separate from one another with no growth occurring until the growth path for the given system is encountered. Once sufficient strain energy is achieved, growth begins with the characteristics of growth depending upon the initial size of the delamination. If $\phi^*_0 < \phi^*_{c1}$ or $\phi^*_0 > \phi^*_{c2}$, growth is catastrophic. If $\phi^*_{c1} < \phi^*_0 < \phi^*_b$, the disbond will grow in an unstable fashion at constant load until the corresponding point on the right hand portion of the well is achieved. Further increases in load cause the delamination to grow in a stable manner following the ascending portion of the well, until the peak is reached. At this point catastrophic growth ensues. If $\phi^*_b \leqslant \phi^*_0 < \phi^*_{c2}$, growth of the disbond is stable followed by catastrophic. For the case of a very weak bond, as discussed earlier, a contact zone may develop after the stable portion of the growth path is encountered.

For a disbond which possesses a contact zone initially, a possible scenario would be as follows; as the load intensity is increased from zero, the corresponding path for that size

disbond is followed (Figs 2 and 3), with the contact zone first expanding and then receding as the sublaminates separate, stretch (compress) and slide in the delaminated region. This process continues until the strain energy is such that eqn (47a) is satisfied, at which point stable growth occurs, as indicated in Figs 2 and 3, until a critical load is achieved and snap-through buckling occurs in the delaminated region. Similarly, if growth has not occurred before the maximum load is achieved, and the load reaches the corresponding maximum, buckling occurs in the delaminated region. At this point, $\phi \to \phi^*$ and growth is governed by eqn (47b). The behavior of the system is then characterized by Figs 4–7 as discussed above, with growth beginning when the corresponding growth path is intercepted.

5. CONCLUDING REMARKS

The problem of debonding of a laminated shell subjected to self-equilibrating line loading has been considered. A self-consistent model has been presented yielding a set of governing equations for the intact portion of the structure and for the sublaminates in the delaminated region of the system. Corresponding boundary and matching conditions, along with transversality conditions defining the variable boundaries of a contact zone and of the delamination, were obtained. It was seen that growth of the disbond was governed by mode II fracture for the case of nonvanishing contact zone, and by a combination of mode I and mode II fracture when the region of separation completely envelops the delamination.

A closed form analytical solution was obtained and numerical simulations were performed demonstrating representative behavior. The system was seen to exhibit relatively complex behavior under the simple loading considered. Characteristics of the system behavior included minimum delamination sizes below which no contact zone exists, snap-through buckling in the delaminated region, and critical delamination sizes separating stable, unstable and catastrophic growth of the disbond. Each of these characteristics was seen to be strongly influenced by the relative stiffnesses of the inner and outer sublaminates, as well as on the strength of the bond, and general trends resulting from these influences were exhibited.

Acknowledgement—This work was supported by a grant from the Center for Computational Modeling of Aircraft Structures (CMAS) at Rutgers University.

REFERENCES

Bottega, W. J. (1983). A growth law for propagation of arbitrary shaped delaminations in layered plates. *Int. J. Solids Structures* **19,** 1009–1017.

Bottega, W. J. (1988a). On thin film delamination growth in a contracting cylinder. *Int. J. Solids Structures* **24,** 13–26.

Bottega, W. J. (1988b). Peeling of a cylindrical layer. *Int. J. Fract.* **38,** 3–14.

Bottega, W. J. (1988c). Debonding of a predeflected segment of layer from the wall of a contracting cavity. *Engng Fract. Mech.* **31,** 1001–1008.

Bottega, W. J. (1988d). On delamination of thin layers from cylindrical surfaces. *Proceedings of the 29th AIAA/ASME/ASCE/AHS Structures, Structural Dynamics and Materials Conference*, pp. 351–358. Williamsburg.

Bottega, W. J. (1990). Instability of a partially delaminated surface layer of an oscillating cylinder. *AIAA J.* **28,** 2008–2011.

Bottega, W. J. (1991). Peeling and bond point propagation in a self-adhered elastica. *Q. J. Mech. Appl. Math.* **44,** 17–33.

Bottega, W. J. (1993). On the separation of concentric elastic rings. *Int. J. Mech. Sci.* **35,** 851–866.

Bottega, W. J. and Maewal, A. (1983a). Delamination buckling and growth in laminates. *ASME J. Appl. Mech.* **50,** 184–189.

Bottega, W. J. and Maewal, A. (1983b). Dynamics of delamination buckling. *Int. J. Nonlin. Mech.* **18,** 449–463.

Bottega, W. J. and Maewal, A. (1983c). Some aspects of delamination buckling and growth in laminates. *Proceedings of the Winter Annual Meeting on Advances in Aerospace Structures, Materials and Dynamics*, pp. 282–290. Boston.

Chang, F.-K. and Kutlu, Z. (1989). Response of composite shells containing a delamination. *Appl. Mech. Rev.* **22,** S48–S53.

Chen, Z. Q. and Simitses, G. J. (1988a). Delamination buckling of pressure-loaded, cross-ply, laminated cylindrical shells. *Z. Angew. Math. Mech.* **10,** 491–501.

Chen, Z. Q. and Simitses, G. J. (1988b). On the postbuckling behavior of a delaminated thin cylindrical shell. In *Composite Structures* 5 (Edited by I. H. Marshall), Chapt. 23, pp. 447–465. Elsevier Applied Science, Oxford.

Kachanov, L. M. (1976). Layering in glass fiber pipes subjected to external pressure. *Mekh. Pol.* **5,** 918–922.

Kachanov, L. M. (1988). *Delamination Buckling of Composite Materials*, Section 1.2, pp. 14–18. Kluwer Academic Publishers.

Kardomateas, G. A. and Chung, C. B. (1992). Thin film modeling of delamination buckling in pressure loaded laminated cylindrical shells. *AIAA J.* **30,** 2119–2123.

Larsson, P.-L. and Leckie, F. A. (1992). Plane strain delamination growth in composite panels. *Compos. Struct.* **20,** 175–184.

Sallam, S. and Simitses, G. J. (1987) Delamination buckling of cylindrical shells under axial compression. *Compos. Struct.* **7,** 83–101.

Simitses, G. J. and Chen, Z. Q. (1988). Buckling of delaminated, long, cylindrical panels under pressure. *Comput. Struct.* **28,** 173–184.

Simitses, G. J., Chen, Z. Q. and Sallam, S. (1991). Delamination buckling in cylindrical laminates. *Thin Walled Struct.* **11,** 25–41.

Troshin, V. P. (1983). Effect of longitudinal delamination in a laminar shell on the critical pressure. *Mekh. Komp. Mat.* **17,** 563–567.

Troshin, V. P. (1993). Use of three-dimensional model of filler in stability problems for triple-layer shells with delaminations. *Mekh. Komp. Mat.* **4,** 657–662.